J. Am. Soc. Mass Spectrom. (2015) 26:934–939
DOI: 10.1007/s13361-015-1119-9

FOCUS: IMAGING MASS SPECTROMETRY: RESEARCH ARTICLE

Pyrylium Salts as Reactive Matrices for MALDI-MS Imaging of Biologically Active Primary Amines

Mohammadreza Shariatgorji,[1] Anna Nilsson,[1] Patrik Källback,[1] Oskar Karlsson,[2,3] Xiaoqun Zhang,[3] Per Svenningsson,[3] Per E. Andren[1]

[1]Biomolecular Imaging and Proteomics, National Center for Mass Spectrometry Imaging, Department of Pharmaceutical Biosciences, Uppsala University, P.O. Box 591 BMC, 75124, Uppsala, Sweden
[2]Drug Safety and Toxicology, Department of Pharmaceutical Biosciences, Uppsala University, P.O. Box 591 BMC, 75124, Uppsala, Sweden
[3]Center for Molecular Medicine, Department of Neurology and Clinical Neuroscience, Karolinska Institutet and Karolinska University Hospital, 17176, Stockholm, Sweden

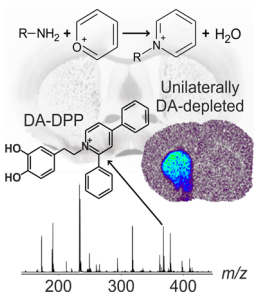

Abstract. Many neuroactive substances, including endogenous biomolecules, environmental compounds, and pharmaceuticals possess primary amine functional groups. Among these are catecholamine neurotransmitters (e.g., dopamine), many substituted phenethylamines (e.g., amphetamine), as well as amino acids and neuropeptides. In most cases, mass spectrometric (ESI and MALDI) analyses of trace amounts of such compounds are challenging because of their poor ionization properties. We present a method for chemical derivatization of primary amines by reaction with pyrylium salts that facilitates their detection by MALDI-MS and enables the imaging of primary amines in brain tissue sections. A screen of pyrylium salts revealed that the 2,4-diphenyl-pyranylium ion efficiently derivatizes primary amines and can be used as a reactive MALDI-MS matrix that induces both derivatization and desorption. MALDI-MS imaging with such matrix was used to map the localization of dopamine and amphetamine in brain tissue sections and to quantitatively map the distribution of the neurotoxin β-*N*-methylamino-L-alanine.

Keywords: MALDI matrix, Mass spectrometry imaging, Neurotransmitter, Catecholamine, Phenethylamine, Amphetamine, Primary amine, Reactive matrix, Neurotoxin

Received: 2 February 2015/Revised: 25 February 2015/Accepted: 25 February 2015/Published Online: 28 March 2015

Introduction

Small organic molecules play vital roles in biological systems, so analytical methods that enable the quantitative and qualitative mapping of such molecules within tissues, organs, and cells are important in several fields of life science research. Many neuroactive small molecules, such as endogenous catecholamine neurotransmitters, exogenous neurotoxins, and pharmaceuticals contain primary amine functional groups.

Matrix-assisted laser desorption ionization (MALDI) is an ionization technique that is used to facilitate analysis by mass spectrometry (MS) in a wide range of research areas [1–4]. MALDI has several advantages over other ionization methods, including softness, high sensitivity, and compatibility with solid samples and diverse mass analyzers. It is, therefore, extremely useful in MS-based studies of biomolecules.

MS imaging (MSI) using MALDI enables label-free mapping of the distributions of molecular species in tissue sections [5]. This technique supports the acquisition of multiplex data without requiring significant a priori information on the chemical species present within the tissue section, and has quickly been established as a powerful in situ visualization tool for imaging, identifying, and quantitating chemical species ranging from alkali metal ions [6] to medium sized polypeptides [7].

Despite its great potential, there are some notable limitations on the applicability of MALDI-MS and MALDI-MSI in the analysis of certain small molecules. First, the matrix compounds that are commonly used in MALDI to facilitate analyte desorption/ionization generate fragment and cluster ions that mask signals of interest in the low molecular weight region (100–600 Da), where most small molecule neurotransmitters

Mohammadreza Shariatgorji and Anna Nilsson contributed equally to this work.

Correspondence to: Per Andren; *e-mail:* per.andren@farmbio.uu.se

and pharmaceuticals are detected. Second, the analysis of less abundant and/or difficult-to-ionize compounds is challenging because of the presence of lipids and other ionization/desorption suppressants, which can dramatically reduce the method's sensitivity toward less abundant compounds.

The simplest way to address the first problem is to use an alternative MALDI matrix [8–10], which will generate a different set of matrix cluster ions that will hopefully not mask the signal of interest. However, different MALDI matrices have different ionization/desorption characteristics and may not enable adequate ionization of the target analyte. More complex techniques and tools have, therefore, been developed, which include nanostructure initiator mass spectrometry (NIMS) [11, 12], ionic matrices [13, 14], desorption ionization from porous silicon (DIOS) [15, 16], and surface-assisted laser desorption ionization [17–19]. Despite some successes, these methods have never been as widely used as conventional MALDI because of technical and practical limitations, some of which are particularly problematic in imaging applications.

The overall sensitivity of MALDI-MSI can be enhanced to some extent by optimizing the type of matrix used, the matrix solvent composition [20], the method of matrix application [21], and the tissue clean up protocol [22], or by chemical derivatization [23–27].

Selective derivatization that adds or stabilizes a charge on the target molecule can enhance the ionization/desorption yield and, hence, the sensitivity of MALDI-MSI analysis. The derivatization reaction should preferably proceed under very mild conditions and rapidly at ambient temperature to preserve the localization of endogenous compounds. Ideally, a derivatizing agent would react rapidly and selectively with the target compound while also functioning as an efficient desorption-promoting matrix.

Pyrylium salts react readily and specifically with primary amines to form pyridinium cations. This property has been exploited to increase the sensitivity of mass spectrometric analyses towards various proteins and small molecules [26, 28, 29].

In this work, we assessed the utility of three different pyrylium salts as derivatizating agents for enhancing the MS sensitivity of primary amine-containing small molecules. Their efficiency was investigated by mapping the distribution of the catecholamine neurotransmitter dopamine (DA) in brain tissue sections, and the best candidate was then used to perform imaging of a substituted phenethylamine (amphetamine) and quantitative MALDI-MSI of the environmental neurotoxin β-*N*-methylamino-L-alanine (L-BMAA) in brain tissue sections.

Methods

Tetrafluoroborate salts of 2,4-diphenyl-pyranylium (DPP), 1,4-phenylene-4,4'-bis (2,6-diphenyl-4-pyrylium) (PBDPP), 2,4,6-trimethylpyrylium (TMP), triethylamine (TEA), and all other chemicals were purchased from Sigma-Aldrich (Stockholm, Sweden) unless otherwise stated and were used without further purification. Water, methanol, and trifluoroacetic acid (TFA) were obtained from Merck (Hohenbrunn, Germany).

Adult Sprague–Dawley rats (190–290 g; BK, Sollentuna, Sweden) were unilaterally lesioned by 6-hydroxydopamine (6-OHDA) as previously described [30]. The animals were killed by decapitation 4 wk after the surgery.

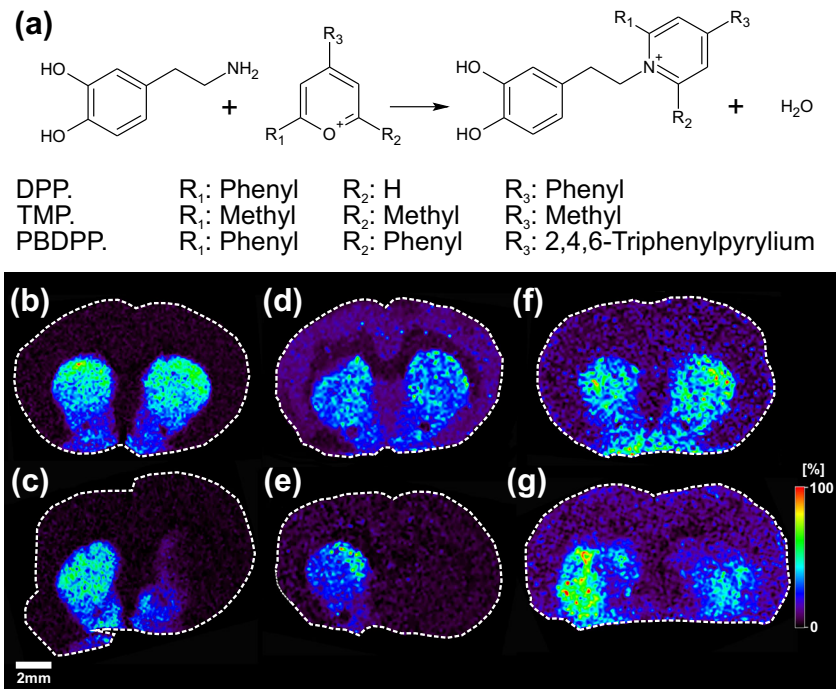

Figure 1. Reaction of dopamine with pyrylium salts (**a**). MALDI-MSI images of DA in coronal tissue sections of control (**b**, **d**, **f**) and unilaterally 6-OHDA lesioned (**c**, **e**, **g**) rat brains after derivatization with DPP (**b**, **c**), PBDPP (**d**, **e**) or TMP (**f**, **g**). Signal intensity is indicated using a rainbow scale. Scale bar: 2 mm; spatial resolution: 120 µm

C57BL/6J male mice (3 mo old, Charles River Lab., Erkrath, Germany) were injected with saline or amphetamine (1 or 5 mg/kg, i.p.) and killed by decapitation 30 min post dose.

Three male Wistar rat pups (Taconic, Ejby, Denmark) were given a sc injection of L-BMAA hydrochloride, 460 mg/kg or 150 mg/kg on postnatal day (PND) 9, and sacrificed by decapitation 8 h post dose [31]. All animal experiments were approved by the local ethical committee (Stockholm and Uppsala) and conducted in accordance with Swedish (Animal Welfare Act SFS1998: 56) and European Union (Convention ETS123 and Directive 86/609/EEC) regulations on animal experimentation. All brains were immediately removed, snap frozen, and stored at –80°C until further analysis. The frozen brain tissues were cut using a cryostat-microtome (Leica CM3050S; Leica Microsystems, Welzlar, Germany) at a thickness of 14 µm, thaw-mounted onto conductive indium tin oxide (ITO) glass slides (Bruker Daltonics), and stored at −80°C. Sections were dried gently under a flow of nitrogen and desiccated at room temperature for 15 min, after which they were imaged optically using a photo scanner (Epson perfection V500). The samples were then coated with derivatization reagents. To enable quantitation, calibration standards of L-BMAA (dissolved in 50% ethanol) were spotted onto a control tissue section prior to derivatization and matrix application.

Stock solutions of DPP (8 mg in 1.2 ml MeOH) and TMP (7 mg in 3 ml MeOH) were prepared and diluted in 6 mL and 4 mL of 70% methanol containing 3.5 µL of TEA, respectively. The PBDPP solution was prepared by directly dissolving 1 mg of the salt in 5 mL of 80% methanol containing 3.5 µL TEA. An automated pneumatic sprayer (TM-Sprayer; HTX Technologies, Carrboro, NC) was used to spray warm reagent over the tissue sections. The nozzle temperature was set at 80°C for DPP and TMP and 70°C for PBDPP, and the reagent was sprayed (80 passes for PBDPP and 30 passes for DPP and TMP) over the tissue sections at a linear velocity of 110 cm/min with a flow rate of about 80 µL/min. Samples were then incubated for 15 min (dried by nitrogen flow every 5 min) in a chamber saturated with vapor from a 50% methanol solution. For TMP-derivatized samples as well as DPP-derivatized L-BMAA, CHCA (5 mg/mL dissolved in 50% ACN containing 0.2% TFA) was applied post derivatization using the automatic sprayer with the following parameters: 6 passes, nozzle temperature 90°C, linear velocity 110 cm/min, flow rate 70 µL/min. All MALDI-MSI experiments were performed using a MALDI-TOF/TOF (Ultraflextreme, Bruker Daltonics, Bremen,

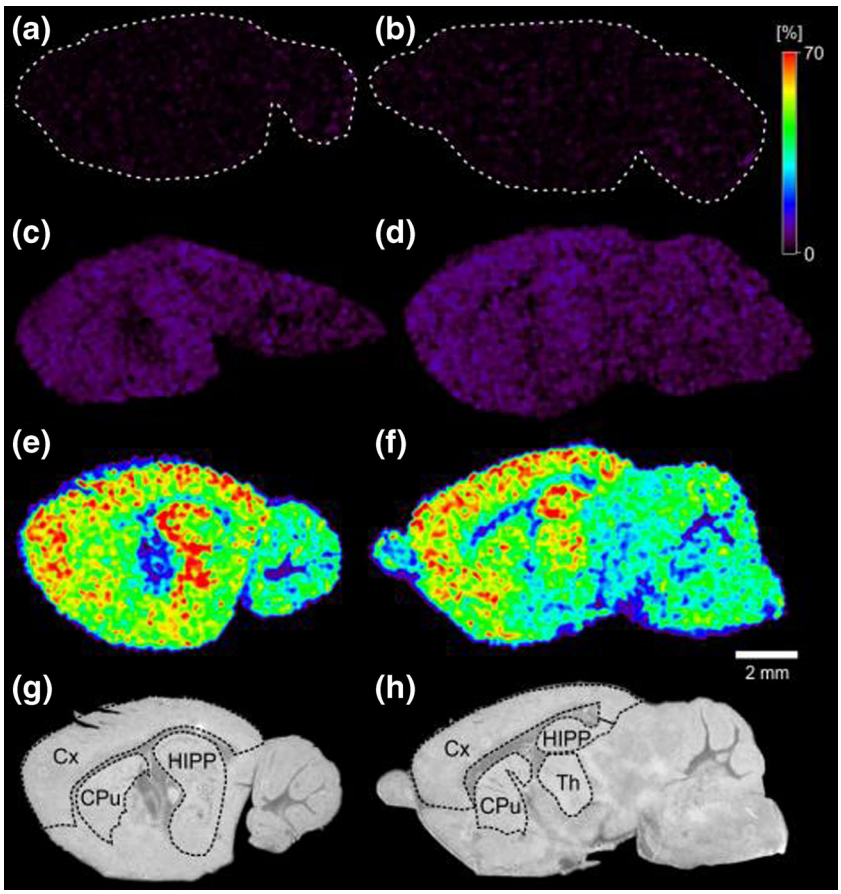

Figure 2. MALDI-MSI of amphetamine (*m/z* 350.2) in sagittal mouse brain tissue sections after derivatization with DPP. Sections were cut from lateral (**a**, **c**, **e**, **g**) and medial (**b**, **d**, **f**, **h**) levels of the brain. Images show the distribution of the peak at *m/z* 350.2 in tissue sections from control animals (**a**, **b**) and animals dosed with amphetamine at 1 mg/kg (**c**, **d**) or 5 mg/kg (**e**, **f**). Scanned images of the sections (**g**, **h**) are also shown, with selected anatomical structures indicated: CPu – Striatum (Caudate-Putamen), Cx – Cortex, HIPP – Hippocampus, Th – Thalamus. Signal intensities are indicated using a rainbow scale. Scale bar: 2 mm; Spatial resolution: 150 µm

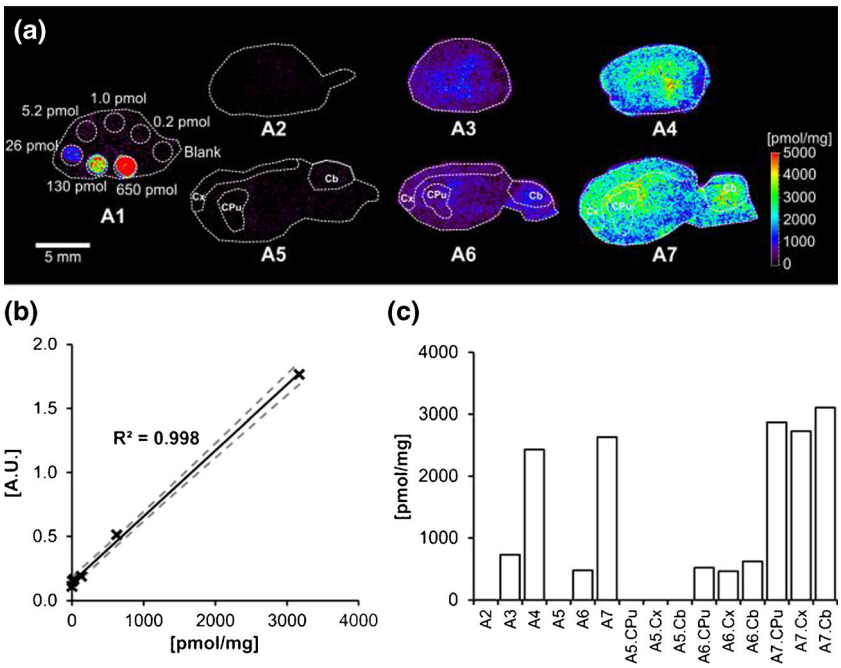

Figure 3. (**a**) Quantitation of L-BMAA following derivatization with DPP. Different amounts of L-BMMA were spotted onto control tissue sections prior to derivatization (A1).The levels of L-BMAA were measured in sagittal sections cut from two different levels of the brains of untreated control animals (A2, A5) and animals dosed with 150 mg/kg (A3, A6) or 460 mg/kg (A4, A7) of L-BMMA. (**b**) Calibration curve obtained using mslQuant (R2=0.998). (**c**) Concentrations of L-BMAA in whole tissue sections and in specific regions of tissue sections A2–A7 from dosed animals. L-BMAA concentrations (in pmol/mg) are indicated using a rainbow scale. Scale bar: 5 mm; spatial resolution: 120 µm. Cx – Cortex, CPu – Striatum (Caudate-Putamen), Cb – Cerebellum

Germany) mass spectrometer with a Smartbeam II 2 kHz laser in positive ion mode. The laser power was optimized at the start of each run and then held constant during the MALDI-MSI experiment. An in-house-developed software package was used for data processing, TIC normalization, visualization, and quantitation. The concentration of L-BMAA in defined regions of interest was calculated by comparing the observed signal intensities to a calibration curve derived from the signals for calibration spots on control tissue sections, assuming a brain tissue density of 1.0 g/cm3.

Results and Discussion

All three of the studied pyrylium salts (DPP, PBDPP, and TMP; Fig. 1a) efficiently derivatized model primary amines in solution. Each reagent contains at least one pyrylium ring but they have different numbers of delocalized electrons and thus different UV-Vis absorption patterns (data not shown) and colors (DPP and PBDPP are yellow; TMP is colorless). Both DPP and PBDPP have relatively high absorptivity at about 355 nm (the wavelength of the laser used in this study) but the absorptivity of TMP in this region is very low. This may be why desorption after TMP derviatization requires the use of CHCA as an assistive matrix whereas acceptable desorption yields are usually achieved when using DPP and PBDPP even without such assistance.

The derivatization reaction that converts primary amines to the corresponding pyrydinium salts occurs at room temperature with no need for heat or extensive incubation, which helps to preserve the localization of molecular species in the sample. To evaluate the efficiency of the pyrylium salts, MALDI-MSI targeting endogenous DA was performed on coronal tissue sections from control and 6-OHDA lesioned animals. This model system was chosen because it is well known that DA is localized in the striatal region of the brain and that 6-OHDA lesioning significantly reduces its concentration in the lesioned side of the brain [26, 32]. Moreover, DA in brain tissue sections is not detectable by MALDI-MSI without chemical modification when using conventional matrices. Both DPP and PBDPP enabled detection of derivatized DA at *m/z* 368.1 (Fig. 1b, c) and *m/z* 692.4 (Fig. 1d, e), respectively, without requiring the use of any additional matrix components. As expected, the highest DA concentrations were observed in the striatal regions of the control hemisphere of the brain tissue section (Fig. 1b, d), and the signal was much less intense in the 6-OHDA lesioned side of the brain (Fig. 1c, e). DPP was considered superior to PBDPP because its solubility allowed it to be used at higher concentrations without causing precipitation or clogging in the sprayer. PBDPP has two pyrylium rings and can potentially react with two primary amines. However, PBDPP-derivatized DA has two positive charges (one of which is counterbalanced by a hydroxide ion), complicating the analysis of its MS data. MS-mode MALDI-MSI analysis using TMP derivatization (in the presence of CHCA) did not enable DA visualization because there was an intense interfering signal at *m/z* 258.1 that overlapped with the expected *m/z* peak for the derivatized amine (data not shown). However, MALDI-MSI analyses in MS/MS mode revealed that the localization patterns of a fragment ion derived from TMP-derivatized DA (*m/z* 137) in

control and 6-OHDA lesioned brain tissue sections (Fig. 1f, g) were similar to those observed in MS mode after DPP- and PBDPP-derivatization.

It is worth noting that DPP forms very small homogeneous crystals, which is crucial when performing high spatial resolution MALDI-MSI. DPP thus enabled high resolution (20 μm) MALDI-MSI of DA in the striatal regions of rat brain tissue sections (data not shown).

To further demonstrate the potential of DPP as a reactive matrix, it was used for on-tissue derivatization and to map the distribution of amphetamine in mouse brain tissue sections from control and dosed animals (Fig. 2). Sagittal sections from two levels of the brain (lateral and medial sections from the midsagittal cut) were analyzed; derivatized amphetamine was detected in most of the brain's structures but mainly in the striatum, hippocampus, and cortex. The overall amphetamine signal intensity in the brains of animals treated with a high dose (5 mg/kg) was about 7.5 times higher than that observed in sections from animals treated with a lower dose (1 mg/kg).

L-BMAA is an important environmental neurotoxin, the poor ionizability of which prevents its molecular imaging using conventional MALDI-MS. Derivatization with DPP quantitatively converted L-BMAA into its diphenyl pyridinium salt, facilitating its desorption, ionization, and quantitative molecular imaging in brain tissue sections. Treatment of the tissue sections with CHCA after derivatization reduced the fragmentation of the derivatized L-BMAA, increasing the sensitivity of the MSI analysis. Quantitative imaging of sagittal tissue sections and selected structures was performed by relating the signals for L-BMAA in dosed animals to those for a calibration curve with adequate linearity (R^2=0.998) constructed by spotting known concentrations of exogenous L-BMAA on a control tissue section. L-BMAA was imaged in tissue sections cut from two levels of the brain and quantified in the whole brain as well as selected structures such as the striatum, cortex and cerebellum (Fig. 3).

In conclusion, three pyrylium salts were found to react efficiently with various bioactive primary amines, enabling sensitive MALDI-MSI and on-tissue quantitation. DPP was shown to be technically and practically advantageous over two alternative reagents (TMS and PBDPP), but either of these agents could be used in cases where DPP is unsuitable, for example because the signal of the DPP-derivatized target amine is obscured by some other endogenous signal.

Acknowledgments

This work was supported by the Swedish Research Council (Medicine and Health 2008-5597, 2013-3105, Natural and Engineering Science 2014-6215, Research Infrastructure 2009-6050) and AstraZeneca, R&D, UK.

References

1. Hillenkamp, F., Peter-Katalinić, J.: MALDI MS: A Practical Guide to Instrumentation, Methods, and Applications, xvi, p. 345. Wiley-VCH, Weinheim (2007)
2. Karas, M., Bachmann, D., Hillenkamp, F.: Influence of the wavelength in high-irradiance ultraviolet-laser desorption mass-spectrometry of organic-molecules. Anal. Chem. **57**, 2935–2939 (1985)
3. van Kampen, J.J., Burgers, P.C., de Groot, R., Gruters, R.A., Luider, T.M.: Biomedical application of MALDI mass spectrometry for small-molecule analysis. Mass Spectrom. Rev. **30**, 101–120 (2011)
4. Webster, J., Oxley, D.: Protein identification by MALDI-TOF mass spectrometry. Methods Mol. Biol. **800**, 227–240 (2012)
5. Cornett, D.S., Reyzer, M.L., Chaurand, P., Caprioli, R.M.: MALDI imaging mass spectrometry: molecular snapshots of biochemical systems. Nat. Methods **4**, 828–833 (2007)
6. Shariatgorji, M., Svenningsson, P., Andren, P.E.: Mass spectrometry imaging, an emerging technology in neuropsychopharmacology. Neuropsychopharmacology **39**, 34–49 (2014)
7. Seeley, E.H., Caprioli, R.M.: Molecular imaging of proteins in tissues by mass spectrometry. Proc. Natl. Acad. Sci. U. S. A. **105**, 18126–18131 (2008)
8. Shanta, S.R., Kim, T.Y., Hong, J.H., Lee, J.H., Shin, C.Y., Kim, K.H., Kim, Y.H., Kim, S.K., Kim, K.P.: A new combination MALDI matrix for small molecule analysis: application to imaging mass spectrometry for drugs and metabolites. Analyst **137**, 5757–5762 (2012)
9. Chen, S., Chen, L., Wang, J., Hou, J., He, Q., Liu, J., Wang, J., Xiong, S., Yang, G., Nie, Z.: 2,3,4,5-Tetrakis(3',4'-dihydroxylphenyl)thiophene: a new matrix for the selective analysis of low molecular weight amines and direct determination of creatinine in urine by MALDI-TOF MS. Anal. Chem. **84**, 10291–10297 (2012)
10. Abdelhamid, H.N., Wu, H.F.: Furoic and mefenamic acids as new matrices for matrix assisted laser desorption/ionization-(MALDI)-mass spectrometry. Talanta **115**, 442–450 (2013)
11. Woo, H.K., Northen, T.R., Yanes, O., Siuzdak, G.: Nanostructure-initiator mass spectrometry: a protocol for preparing and applying NIMS surfaces for high-sensitivity mass analysis. Nat. Protoc. **3**, 1341–1349 (2008)
12. Greving, M.P., Patti, G.J., Siuzdak, G.: Nanostructure-initiator mass spectrometry metabolite analysis and imaging. Anal. Chem. **83**, 2–7 (2011)
13. Shrivas, K., Hayasaka, T., Goto-Inoue, N., Sugiura, Y., Zaima, N., Setou, M.: Ionic matrix for enhanced MALDI imaging mass spectrometry for identification of phospholipids in mouse liver and cerebellum tissue sections. Anal. Chem. **82**, 8800–8806 (2010)
14. Li, Y.L., Gross, M.L.: Ionic-liquid matrices for quantitative analysis by MALDI-TOF mass spectrometry. J. Am. Soc. Mass Spectrom. **15**, 1833–1837 (2004)
15. Wei, J., Buriak, J.M., Siuzdak, G.: Desorption-ionization mass spectrometry on porous silicon. Nature **399**, 243–246 (1999)
16. Ronci, M., Rudd, D., Guinan, T., Benkendorff, K., Voelcker, N.H.: Mass spectrometry imaging on porous silicon: investigating the distribution of bioactives in marine molluscs tissues. Anal. Chem. **84**, 8996–9001 (2012)
17. Kawasaki, H., Ozawa, T., Hisatomi, H., Arakawa, R.: Platinum vapor deposition surface-assisted laser desorption/ionization for imaging mass spectrometry of small molecules. Rapid Commun. Mass Spectrom. **26**, 1849–1858 (2012)
18. Guinan, T., Kirkbride, P., Pigou, P.E., Ronci, M., Kobus, H., Voelcker, N.H.: Surface-assisted laser desorption ionization mass spectrometry techniques for application in forensics. Mass Spectrom. Rev. doi: 10.1002/mas.21431 (2014)
19. Alhmoud, H.Z., Guinan, T.M., Elnathan, R., Kobus, H., Voelcker, N.H.: Surface-assisted laser desorption/ionization mass spectrometry using ordered silicon nanopillar arrays. Analyst **139**, 5999–6009 (2014)
20. Schwartz, S.A., Reyzer, M.L., Caprioli, R.M.: Direct tissue analysis using matrix-assisted laser desorption/ionization mass spectrometry: practical aspects of sample preparation. J. Mass Spectrom. **38**, 699–708 (2003)
21. Gemperline, E., Rawson, S., Li, L.: Optimization and comparison of multiple MALDI matrix application methods for small molecule mass spectrometric imaging. Anal. Chem. **86**, 10030–10035 (2014)
22. Shariatgorji, M., Kallback, P., Gustavsson, L., Schintu, N., Svenningsson, P., Goodwin, R.J., Andren, P.E.: Controlled-pH tissue cleanup protocol for signal enhancement of small molecule drugs analyzed by MALDI-MS imaging. Anal. Chem. **84**, 4603–4607 (2012)
23. Chacon, A., Zagol-Ikapitte, I., Amarnath, V., Reyzer, M.L., Oates, J.A., Caprioli, R.M., Boutaud, O.: On-tissue chemical derivatization of 3-methoxysalicylamine for MALDI-imaging mass spectrometry. J. Mass Spectrom. **46**, 840–846 (2011)
24. Toue, S., Sugiura, Y., Kubo, A., Ohmura, M., Karakawa, S., Mizukoshi, T., Yoneda, J., Miyano, H., Noguchi, Y., Kobayashi, T., Kabe, Y., Suematsu, M.: Microscopic imaging mass spectrometry assisted by on-tissue chemical

derivatization for visualizing multiple amino acids in human colon cancer xenografts. Proteomics **14**, 810–819 (2014)
25. Manier, M.L., Spraggins, J.M., Reyzer, M.L., Norris, J.L., Caprioli, R.M.: A derivatization and validation strategy for determining the spatial localization of endogenous amine metabolites in tissues using MALDI imaging mass spectrometry. J. Mass Spectrom. **49**, 665–673 (2014)
26. Shariatgorji, M., Nilsson, A., Goodwin, R.J., Kallback, P., Schintu, N., Zhang, X., Crossman, A.R., Bezard, E., Svenningsson, P., Andren, P.E.: Direct targeted quantitative molecular imaging of neurotransmitters in brain tissue sections. Neuron **84**, 697–707 (2014)
27. Cobice, D.F., Mackay, C.L., Goodwin, R.J., McBride, A., Langridge-Smith, P.R., Webster, S.P., Walker, B.R., Andrew, R.: Mass spectrometry imaging for dissecting steroid intracrinology within target tissues. Anal. Chem. **85**, 11576–11584 (2013)
28. O'Leary, M.H., Samberg, G.A.: Chemical modification of proteins by pyrylium salts. J. Am. Chem. Soc. **93**, 3530–3532 (1971)
29. Johannesen, S.A., Beeren, S.R., Blank, D., Yang, B.Y., Geyer, R., Hindsgaul, O.: Glycan analysis via derivatization with a fluorogenic pyrylium dye. Carbohydr. Res. **352**, 94–100 (2012)
30. Zhang, X., Andren, P.E., Chergui, K., Svenningsson, P.: Neurokinin B/NK3 receptors exert feedback inhibition on L-DOPA actions in the 6-OHDA lesion rat model of Parkinson's disease. Neuropharmacology **54**, 1143–1152 (2008)
31. Karlsson, O., Berg, A.L., Lindstrom, A.K., Hanrieder, J., Arnerup, G., Roman, E., Bergquist, J., Lindquist, N.G., Brittebo, E.B., Andersson, M.: Neonatal exposure to the cyanobacterial toxin BMAA induces changes in protein expression and neurodegeneration in adult hippocampus. Toxicol. Sci. **130**, 391–404 (2012)
32. Chotibut, T., Apple, D.M., Jefferis, R., Salvatore, M.F.: Dopamine transporter loss in 6-OHDA Parkinson's model is unmet by parallel reduction in dopamine uptake. PLoS One **7**, e52322 (2012)